Received: 17 November 2022 | Revised: 1 June 2023 | Accepted: 19 June 2023

DOI: 10.1002/mma.9520

RESEARCH ARTICLE

WILEY

The boundary integral equation describing a curvilinear solid/liquid interface with nonlinear phase transition temperature

E. A. Titova[1] | **A. A. Ivanov**[1] | **L. V. Toropova**[2,3]

[1]Laboratory of Multi?Scale Mathematical Modeling, Department of Theoretical and Mathematical Physics, Ural Federal University, Ekaterinburg, Russian Federation

[2]Laboratory of Mathematical Modeling of Physical and Chemical Processes in Multiphase Media, Department of Theoretical and Mathematical Physics, Ural Federal University, Ekaterinburg, Russian Federation

[3]Otto-Schott-Institut für Materialforschung, Friedrich-Schiller-Universität-Jena, Jena, Germany

Correspondence
L. V. Toropova, Laboratory of Mathematical Modeling of Physical and Chemical Processes in Multiphase Media, Department of Theoretical and Mathematical Physics, Ural Federal University, Lenin Avenue, 51, Ekaterinburg 620000, Russian Federation.
Email: l.v.toropova@urfu.ru

Communicated by: I. Nizovtseva

Funding information
Ministry of Science and Higher Education of the Russian Federation (project 075-02-2023-935 for the "Ural Mathematical Center"); Foundation for the Advancement of Theoretical Physics and Mathematics "BASIS": 21-1-3-11-1.

The boundary integral equation (BIE) describes the dynamics of a curved crystallization front separating liquid melt and solid material. We derive a generalized BIE for the thermal-concentration problem taking into account the nonlinear dependence of the crystallization temperature on solute concentration and the kinetics of atomic attachment at the interface. This equation determines the evolution of the interface function and the equation for crystallization driving force - the melt undercooling at the crystal surface. Our calculations carried out for a dendritic vertex in the form of a paraboloid of revolution have shown that the growth rate of the dendritic tip and its diameter substantially depend on the nonlinear effects under study. In particular, the velocity and diameter of the dendrite tip respectively become greater and narrower with increasing deviation of the liquidus equation from the linear relationship. Also, the dendrite tip velocity can be significantly affected by variations in the exponent of atomic kinetics.

KEYWORDS

boundary integral equation, curved solid-liquid interfaces, phase transitions, undercooled melts

MSC CLASSIFICATION

80A19, 80A22

1 | INTRODUCTION

The evolution of the curvilinear liquid-solid interface in the crystallization processes of undercooled melts and supersaturated solutions is responsible for the properties of solidifying materials [1–9]. Thus, for example, the crystallization front displaces a part of the dissolved impurity into the liquid phase and another part of the impurity is absorbed into

E. A. Titova and L. V. Toropova contributed equally to this work.

the solid material during this process. Thus, the melt immediately upstream of the front is enriched with impurity. As the impurity concentration increases, however, the crystallization temperature of the liquid decreases and a significantly lower temperature may be required to solidify certain liquid regions ahead of the front. If we pay our attention to the well-known example of seawater freezing, ice almost completely displaces all the salt into the water and greatly increases its salinity. Consequently, regions of unfrozen, extremely saline seawater remain in frozen ice even in wintertime, as such regions require very low temperatures to freeze. Moreover, the interface dynamics are also responsible for the morphological instability [10–14], the formation of a two-phase concentration undercooling region [15–19], the structure in the solid phase material (layered impurity liquation, impurity cells, grain and dendritic microstructure) [2, 20–23].

In 1974, Nash and Glicksman [24, 25] proposed a method to determine the boundary integral equation (BIE) for the interface function defining the curvilinear crystallization front for the thermal problem. This Green's function based method was then extended by Langer, Turski, Alexandrov, Galenko and Titova to describe the interface motion in solid-liquid, solid-solid and liquid-liquid systems [26–29]. A generalization of the BIE to crystallization of undercooled binary melts with convection has been made by Saville, Beaghton, Titova, and Alexandrov [30–32]. Recently, the BIE has been derived for a rapid solidification process where the concentration field in the liquid is described by a diffusion equation of hyperbolic type, which takes the jump time of atoms to neighboring vacant positions into account [33]. Note that the BIE approach can be used to derive a criterion for stable dendritic growth [34, 35], as well as for numerical simulation of the shapes of growing patterns that arise in crystallization processes from undercooled melts [29].

In this paper, we extend the BIE theory to the case of nonlinear dependence of the phase transformation temperature on dissolved impurity concentration and the kinetics of atoms attachment to the interfacial boundary. As shown below, both these effects essentially modify the equation for the interface function in the case of crystallization with arbitrary curvilinear fronts as well as the basic controlling dependences “dendrite tip velocity - melt undercooling” and “dendrite tip diameter - melt undercooling” in the case of dendrite crystal growth.

2 | MODEL AND INTERFACE FUNCTION

In this section, we represent the initial moving-boundary heat and mass transfer problem with allowance for a nonlinear liquidus equation due to the quadratic dependence of phase transition temperature on impurity concentration and power law of atomic kinetics. Using this model, we derive the BIE for the interface function and an equation for the process driving force - melt undercooling. Analyzing this undercooling for the 3D dendritic crystal, we show the effects of nonlinear terms of the liquidus equation.

2.1 | An arbitrary shape reference frame

We consider the three-dimensional crystallization process with a curvilinear solid-liquid phase interface (front) illustrated in Figure 1. The heat transfer equation for the liquid-solid (bulk) phases and the solute diffusion equation in the liquid phase can be written as

$$\frac{\partial T'}{\partial t'} + (\mathbf{u}\cdot\nabla)T' - V\frac{\partial T'}{\partial z'} = D_T\nabla^2 T', \tag{1}$$

$$\frac{\partial C'}{\partial t'} + (\mathbf{u}\cdot\nabla)C' - V\frac{\partial C'}{\partial z'} = D_C\nabla^2 C', \tag{2}$$

where T' is the temperature, C' is the solute concentration, $\mathbf{u}$ is the arbitrary fluid velocity, D_T is the thermal conductivity, D_C is the diffusion coefficient, and V is the constant velocity of Cartesian coordinate system (x', y', z') (steady-state growth rate).

The temperature, solute concentration, and fluid velocity are fixed far from the phase transition interface, $T' = T'_\infty,\ C' = C'_\infty,\ \mathbf{u} = U_\infty$, and the boundary conditions at the solid/liquid interface take the form

$$\begin{aligned} T'_i &= T'_0 - d_c\mathcal{K}'\frac{Q}{c_p} + m_1C'_i + m_2C'^2_i - \beta_k\left(V + \frac{\partial\zeta'}{\partial t'}\right)^n,\ \mathbf{u} = 0,\\ D_T\left(\nabla T'_{solid} - \nabla T'_{liquid}\right)\cdot d\mathbf{s}' &= \frac{Q}{c_p}\left(V + \frac{\partial\zeta'}{\partial t'}\right)d^2x',\\ -D_C\nabla C'\cdot d\mathbf{s}' &= (1-k_0)C'_i\left(V + \frac{\partial\zeta'}{\partial t'}\right)d^2x', \end{aligned} \tag{3}$$

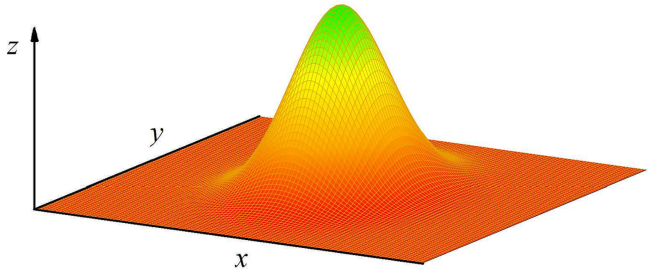

FIGURE 1 The phase-transition interface dividing pure solid (lower part) and pure liquid (upper part) phases. [Colour figure can be viewed at wileyonlinelibrary.com]

where d_c is the anisotropy capillary length, $\mathcal{K}'$ is the average interface curvature, Q is the latent heat of crystallization, m_1 is the linear term of liquidus slope and m_2 is the coefficient of deviation of the liquidus equation from a linear form [36], c_p is the heat capacity, β_k is the kinetic coefficient, n is the kinetic power, T_0' is the phase transition temperature for the flat front, $d\mathbf{s}'$ is the surface area vector element directed toward the liquid phase, k_0 is the solute partition coefficient, ζ' is the interface function, T_i' and C_i' are the interfacial temperature and impurity concentration, respectively. The average curvature of the interface $\mathcal{K}'$ in three-dimensional case can be determined as

$$\mathcal{K}'(\mathbf{x}', t') = -\nabla \cdot \left[\frac{\nabla \zeta'(\mathbf{x}', t')}{\sqrt{1 + (\nabla \zeta'(\mathbf{x}', t'))^2}} \right]. \tag{4}$$

Below we derive an integro-differential equation for the dimensionless interface function $\zeta(\mathbf{x}, t)$ in the case of thermo-diffusion problem with convection (1)–(4). For convenience, let us introduce the characteristic length $2D_T/V$ and time $4D_T/V^2$ scales as well as dimensionless temperatures $T = T'c_p/Q$, solute concentration $C = m_1 c_p C'/Q$, kinetic coefficient $\beta = \beta_k c_p V^n/(2^n Q)$, and fluid velocity $\mathbf{v} = \mathbf{u}/U_\infty$. Note that prime symbol is used for dimensional parameters.

Thus, the dimensionless model of convective heat and mass transfer follows from (1), (3) and has the form

$$\frac{\partial T}{\partial t} + 2\frac{U_\infty}{V}(\mathbf{v} \cdot \nabla)T - 2\frac{\partial T}{\partial z} - \nabla^2 T = 0, \tag{5}$$

$$\frac{\partial C}{\partial t} + 2\frac{U_\infty}{V}(\mathbf{v} \cdot \nabla)C - 2\frac{\partial C}{\partial z} - \frac{D_C}{D_T}\nabla^2 C = 0, \tag{6}$$

$$T_i = T_0 - \frac{d_c K V}{2D_T} + C_i + \frac{Q m_2}{m_1^2 c_p} C_i^2 - \beta\left(2 + \frac{\partial \zeta}{\partial t}\right)^n \text{ at } \zeta, \tag{7}$$

$$(\nabla T_s - \nabla T_l) \cdot d\mathbf{s} = \left(2 + \frac{\partial \zeta}{\partial t}\right) d^2x \text{ at } \zeta, \tag{8}$$

$$-\frac{D_C}{D_T}\nabla C_l \cdot d\mathbf{s} = (1 - k_0)C_i \left(2 + \frac{\partial \zeta}{\partial t}\right) d^2x \text{ at } \zeta, \tag{9}$$

$$T = T_\infty, \ C = C_\infty, \ \mathbf{v} = 1 \text{ at infinity}, \tag{10}$$

where ζ denotes the liquid-solid interface, and subscript i corresponds to the interface.

We use the Green's functions $G_T(\mathbf{p}|\mathbf{p}_1)$ for heat conduction equation and $G_C(\mathbf{p}|\mathbf{p}_1)$ for diffusion equation without flow to solve the convective problem (5)–(10)

$$\frac{\partial G_T}{\partial t_1} + \nabla_1^2 G_T - 2\frac{\partial G_T}{\partial z_1} = -\delta(\mathbf{p} - \mathbf{p}_1), \ \frac{\partial G_C}{\partial t_1} + \frac{D_C}{D_T}\nabla_1^2 G_C - 2\frac{\partial G_C}{\partial z_1} = -\delta(\mathbf{p} - \mathbf{p}_1), \tag{11}$$

where $\mathbf{p} = (\mathbf{x}, z, t)$, $\mathbf{p}_1 = (\mathbf{x}_1, z_1, t_1)$, $\mathbf{x} = (x, y)$, and $\mathbf{x}_1 = (x_1, y_1)$. The Green's functions for heat $G_T(\mathbf{p}|\mathbf{p}_1)$ and mass $G_C(\mathbf{p}|\mathbf{p}_1)$ transfer problems can be obtained using the Fourier transforms (see, among others, previous works [26–28, 37]) and read as

$$G_T(\mathbf{p}|\mathbf{p}_1) = \left(\frac{1}{4\pi(t-t_1)}\right)^{3/2} \exp\left(-\frac{|\mathbf{x}-\mathbf{x}_1|^2 + [z - z_1 + 2(t-t_1)]^2}{4(t-t_1)}\right), \tag{12}$$

$$G_C(\mathbf{p}|\mathbf{p}_1) = \left(\frac{D_T}{4\pi(t-t_1)D_C}\right)^{3/2} \exp\left(-D_T\frac{|\mathbf{x}-\mathbf{x}_1|^2 + (z - z_1 + 2(t-t_1))^2}{4(t-t_1)D_C}\right). \tag{13}$$

By multiplying Equations (5) and (6) at the point $\mathbf{p}_1$ by $G_T(\mathbf{p}|\mathbf{p}_1)$ and $G_C(\mathbf{p}, \mathbf{p}_1)$, Equation (11) by $T(\mathbf{p}_1)$ and $C(\mathbf{p}_1)$, respectively, subtracting one from the other and integrating the result over $\mathbf{p}_1$, we obtain

$$\begin{aligned} T(\mathbf{p}) = &\int_{-\infty}^{t+\varepsilon}\int_{\Lambda_1} dt_1 dx_1 dy_1 dz_1 \left(2\frac{\partial(G_T T)}{\partial z_1} - 2G_T\frac{U_\infty}{V}(\mathbf{v}\cdot\nabla_1)T - \frac{\partial(G_T T)}{\partial t_1}\right) \\ &+ \int_{-\infty}^{t+\varepsilon}\int_{\Lambda_1} dt_1 dx_1 dy_1 dz_1 \left(G_T\nabla_1^2 T - T\nabla_1^2 G_T\right), \end{aligned} \tag{14}$$

$$\begin{aligned} C(\mathbf{p}) = &\int_{-\infty}^{t+\varepsilon}\int_{\Lambda_1} dt_1 dx_1 dy_1 dz_1 \left(2\frac{\partial(G_C C)}{\partial z_1} - 2G_C\frac{U_\infty}{V}(\mathbf{v}\cdot\nabla_1)C - \frac{\partial(G_C C)}{\partial t_1}\right) \\ &+ \frac{D_C}{D_T}\int_{-\infty}^{t+\varepsilon}\int_{\Lambda_1} dt_1 dx_1 dy_1 dz_1 \left(G_C\nabla_1^2 C - C\nabla_1^2 G_C\right), \end{aligned} \tag{15}$$

where Λ_1 is the volume containing the point (x, y, z), and ε represents small positive parameter.

The integral of the time derivative in Equations (14) and (15) turns to zero after integration over time t_1. In this case, the Green function tends to zero and the temperature and concentration are bounded at the lower limit of integration. Moreover, the Green's function is equal to zero at the upper limit because of the causality condition [26, 28]. In addition, the integral of the z_1-derivative over z_1 in expressions (14) and (15) gives constant temperature T_∞ and concentration C_∞. Next, applying Green's theorem, substituting the heat and mass boundary conditions (7)–(10) into (16) and (17) and extending the point $\mathbf{p}$ to the phase transition surface and taking $\varepsilon \to 0$, we arrive at

$$\int_{-\infty}^{t}\int_{-\infty}^{\infty}\int_{-\infty}^{\infty} dt_1 dx_1 dy_1 \left(G_T(\mathbf{p}^\zeta|\mathbf{p}_1^\zeta)\left(2 + \frac{\partial\zeta}{\partial t}\right)\right) - 2\frac{U_\infty}{V}\int_{-\infty}^{t}\int_{\Lambda_1} (G_T(\mathbf{v}\cdot\nabla_1)T)\, dt_1 dx_1 dy_1 dz_1 = T_i - T_\infty, \tag{16}$$

$$(1-k_0)\int_{-\infty}^{t}\int_{-\infty}^{\infty}\int_{-\infty}^{\infty} dt_1 dx_1 dy_1 \left(C_i G_C(\mathbf{p}^\zeta|\mathbf{p}_1^\zeta)\left(2 + \frac{\partial\zeta}{\partial t}\right)\right) - 2\frac{U_\infty}{V}\int_{-\infty}^{t}\int_{\Lambda_1} (G_C(\mathbf{v}\cdot\nabla_1)C)\, dt_1 dx_1 dy_1 dz_1 = C_i - C_\infty. \tag{17}$$

Expressing the interfacial temperature from the boundary integral equation (16) and substituting it into the Gibbs–Thomson relation (7), we get

$$\begin{aligned} &\int_{-\infty}^{t}\int_{-\infty}^{\infty}\int_{-\infty}^{\infty} dt_1 dx_1 dy_1 \left(G_T(\mathbf{p}^\zeta|\mathbf{p}_1^\zeta)\left(2 + \frac{\partial\zeta}{\partial t}\right)\right) \\ &- 2\frac{U_\infty}{V}\int_{-\infty}^{t}\int_{\Lambda_1} (G_T(\mathbf{v}\cdot\nabla_1)T)\, dt_1 dx_1 dy_1 dz_1 = \Delta - \frac{d_c K V}{2D_T} + C_i + \frac{Q m_2}{m_1^2 c_p}C_i^2 - \beta\left(2 + \frac{\partial\zeta}{\partial t}\right)^n. \end{aligned} \tag{18}$$

The interfacial concentration C_i is given by (17). Thus, expression (18) represents an integro-differential equation for the interface function $\zeta(\mathbf{x}, t)$ satisfying the convective problem (5)–(10) and describing the dynamics of the interface function for the heat and chemical problem with convection.

2.2 | Stationary growth

During stationary growth, the dendrite retains its shape, which means that its surface is isothermal and has the same chemical composition. Then we can take the constant C_i out of the integral in (17) and CBIE (18) and (17) transform to

$$2\int_{-\infty}^{t}\int_{-\infty}^{\infty}\int_{-\infty}^{\infty} G_T(\mathbf{p}^{\zeta}|\mathbf{p}_1^{\zeta})dt_1dx_1dy_1 - 2\frac{U_\infty}{V}\int_{-\infty}^{t}\int_{\Lambda_1}(G_T(\mathbf{v}\cdot\nabla_1)T)\,dt_1dx_1dy_1dz_1 = \Delta - \frac{d_cKV}{2D_T} + C_i + \frac{Qm_2}{m_1^2c_p}C_i^2 - 2^n\beta, \tag{19}$$

$$C_i = \frac{2\frac{U_\infty}{V}\int_{-\infty}^{t}\int_{\Lambda_1}(G_C(\mathbf{v}\cdot\nabla_1)C)\,dt_1dx_1dy_1dz_1 - C_\infty}{2(1-k_0)C_i\int_{-\infty}^{t}\int_{-\infty}^{\infty}\int_{-\infty}^{\infty} G_C(\mathbf{p}^{\zeta}|\mathbf{p}_1^{\zeta})dt_1dx_1dy_1 - 1}. \tag{20}$$

In the stationary case, only the Green's functions depend on time. We now consider how to integrate the thermal Green's function over time. In the stationary case, z and z_1 are independent of time that leads to

$$\int_{-\infty}^{t} G_T(\mathbf{p}^{\zeta}|\mathbf{p}_1^{\zeta})dt_1 = \exp(z_1-z)\left(\frac{1}{4\pi}\right)^{3/2}\sqrt{2}\int_0^{\infty}\exp\left(-\frac{1}{2}\left[\frac{|\mathbf{x}-\mathbf{x}_1|^2+[z-z_1]^2}{\tau}+\tau\right]\right)\frac{d\tau}{\tau^{3/2}}, \tag{21}$$

where $\tau = 2(t-t_1)$. The integral in (21) can be reduced to a modified Bessel function $K_{1/2}$ [38]

$$\int_{-\infty}^{t} G_T(\mathbf{p}^{\zeta}|\mathbf{p}_1^{\zeta})dt_1 = \exp(z_1-z)\left(\frac{1}{2\pi}\right)^{3/2}\frac{K_{1/2}\left(\sqrt{|\mathbf{x}-\mathbf{x}_1|^2+[z-z_1]^2}\right)}{\left(|\mathbf{x}-\mathbf{x}_1|^2+[z-z_1]^2\right)^{1/4}}. \tag{22}$$

Similarly, we can integrate over time the concentration Green's function. The result reads as

$$\int_{-\infty}^{t} G_C(\mathbf{p}^{\zeta}|\mathbf{p}_1^{\zeta})dt_1 = \exp\left(\frac{z_1-z}{D_C/D_T}\right)\left(\frac{D_T}{2\pi D_C}\right)^{3/2}\frac{K_{1/2}\left(\frac{D_T}{D_C}\sqrt{|\mathbf{x}-\mathbf{x}_1|^2+[z-z_1]^2}\right)}{\left(|\mathbf{x}-\mathbf{x}_1|^2+[z-z_1]^2\right)^{1/4}}. \tag{23}$$

Substituting time integrals (22) and (23) into the CBIE (19) and (20), we have

$$\begin{aligned}&\frac{1}{\sqrt{2}\pi^{3/2}}\int_{-\infty}^{\infty}\int_{-\infty}^{\infty}\exp(\zeta_1-\zeta)\frac{K_{1/2}\left(\sqrt{|\mathbf{x}-\mathbf{x}_1|^2+[\zeta-\zeta_1]^2}\right)}{\left(|\mathbf{x}-\mathbf{x}_1|^2+[\zeta-\zeta_1]^2\right)^{1/4}}dx_1dy_1 - \Delta + \frac{d_cKV}{2D_T} - C_i - \frac{Qm_2}{m_1^2c_p}C_i^2 + 2^n\beta\\ &= \frac{U_\infty}{V}\frac{1}{\sqrt{2}\pi^{3/2}}\int_{-\infty}^{\infty}\int_{-\infty}^{\infty}\int_{\zeta}^{\infty}\left(\exp(z_1-\zeta)\frac{K_{1/2}\left(\sqrt{|\mathbf{x}-\mathbf{x}_1|^2+[\zeta-z_1]^2}\right)}{\left(|\mathbf{x}-\mathbf{x}_1|^2+[\zeta-z_1]^2\right)^{1/4}}(\mathbf{v}\cdot\nabla_1)T\right)dx_1dy_1dz_1,\end{aligned} \tag{24}$$

$$C_i = \frac{\frac{U_\infty}{V}\left(\frac{D_T}{\pi D_C}\right)^{3/2}\int_{-\infty}^{\infty}\int_{-\infty}^{\infty}\int_{\zeta}^{\infty}\left(\exp\left(\frac{z_1-\zeta}{D_C/D_T}\right)\frac{K_{1/2}\left(\frac{D_T}{D_C}\sqrt{|\mathbf{x}-\mathbf{x}_1|^2+[\zeta-z_1]^2}\right)}{\left(|\mathbf{x}-\mathbf{x}_1|^2+[\zeta-z_1]^2\right)^{1/4}}(\mathbf{v}\cdot\nabla_1)C\right)dx_1dy_1dz_1 - \sqrt{2}C_\infty}{(1-k_0)C_i\left(\frac{D_T}{\pi D_C}\right)^{3/2}\int_{-\infty}^{\infty}\int_{-\infty}^{\infty}\exp\left(\frac{\zeta_1-\zeta}{D_C/D_T}\right)\frac{K_{1/2}\left(\frac{D_T}{D_C}\sqrt{|\mathbf{x}-\mathbf{x}_1|^2+[\zeta-\zeta_1]^2}\right)}{\left(|\mathbf{x}-\mathbf{x}_1|^2+[\zeta-\zeta_1]^2\right)^{1/4}}dx_1dy_1 - \sqrt{2}}. \tag{25}$$

2.3 | The paraboloid of revolution reference frame

In Equations (17) and (18), the integrals of Green's function over crystal surface were calculated in previous work [28] for the case of thermo-chemical dendrite growth without convection, the result is

$$2\int_{-\infty}^{t}\int_{-\infty}^{\infty}\int_{-\infty}^{\infty} G(\mathbf{p}^{\zeta}|\mathbf{p}_1^{\zeta})dt_1 = p\exp(p)\int_{p}^{\infty}\frac{\exp(-x)}{x}dx, \tag{26}$$

where $p = p_T = \rho V/(2D_T)$ and $p = p_C = \rho V/(2D_C)$ for the thermal and chemical Green's functions, respectively; and ρ is the crystal tip diameter. To calculate the convective terms, we replace the variable z from Equations (17) and (18) with the variable w defining the isotherms

$$z = \frac{p_T w}{2} - \frac{x^2+y^2}{2p_T w}. \tag{27}$$

Note that $w = 1$ corresponds to a dendritic surface and $\zeta = z(w = 1)$. Replacing the variables in (18), we come to

$$\begin{aligned} &p_T\exp(p_T)\int_{p_T}^{\infty}\frac{\exp(-x)}{x}dx - \Delta + \frac{d_c K V}{2D_T} - C_i - \frac{Qm_2}{m_1^2 c_p}C_i^2 + 2^n\beta \\ &= \frac{U_\infty}{p_T V}\int_{-\infty}^{t}\int_{-\infty}^{\infty}\int_{-\infty}^{\infty}\int_{1}^{\infty}\left(G_T(\mathbf{v}\cdot\nabla_1 T)\frac{p_T^2 w_1^2 - x_1^2 - y_1^2}{w_1^2}\right)dt_1 dx_1 dy_1 dw_1. \end{aligned} \tag{28}$$

The concentration convective integral contribution has the same form. The next step of our analysis is to obtain the temperature gradient

$$(\mathbf{v}\cdot\nabla_1 T) = \frac{2w_1 v_w}{\sqrt{p_T^2 w_1^2 + x_1^2 + y_1^2}}\frac{dT}{dw_1}. \tag{29}$$

To obtain dT/dw_1, let us rewrite the heat conduction equation in parabolic coordinates. Since the temperature depends only on one variable w, we obtain

$$\frac{dT}{dw} = -\frac{p_T}{\sqrt{w}}\exp\left(p_T\int_{1}^{w}(v_2(w_2))\,dw_2 + p_T(1-w)\right). \tag{30}$$

The hydrodynamic field was found in Dash and Gill [39] and reads as

$$v_2(w) = \frac{U_\infty}{V}\frac{\sqrt{p_T^2 w^2 + x^2 + y^2}}{p_T w}v_w = \frac{2U_\infty}{wVRe}\frac{\exp(-Re/2) - \exp(-Rew/2)}{E_1(Re/2)} - \frac{U_\infty}{V} + \frac{U_\infty}{V}\frac{E_1(Rew/2)}{E_1(Re/2)}, \tag{31}$$

where $Re = \rho U/\nu$ is the Reynolds number, ν is the kinematic viscosity and

$$E_1(w) = \int_{w}^{\infty}\frac{\exp(-Rew/2)}{w}dw. \tag{32}$$

By substituting the temperature gradient in Equation (33), we arrive at

$$\begin{aligned} &p_T \exp(p_T) \int_{p_T}^{\infty} \frac{\exp(-x)}{x} dx - \Delta + \frac{d_c K V}{2D_T} - C_i - \frac{Q m_2}{m_1^2 c_p} C_i^2 + 2^n \beta \\ &= 2p_T \int_{-\infty}^{t} \int_{-\infty}^{\infty} \int_{-\infty}^{\infty} \int_{1}^{\infty} \left(G_T v_2(w_1) \exp\left(p_T \int_{1}^{w_1} (v_2(w_2))\, dw_2 + p_T(1 - w_1) \right) \right) dt_1 dx_1 dy_1 \frac{dw_1}{w_1}. \end{aligned} \tag{33}$$

Here, we can see that only the Green's function depends on x_1, y_1 and t_1. By integrating the Green's function over these variables, we obtain [28]

$$\int_{-\infty}^{t} \int_{-\infty}^{\infty} \int_{-\infty}^{\infty} G_T(\mathbf{p}^{\zeta} | \mathbf{p}_1) dt_1 dx_1 dy_1 = \frac{p_T w_1}{2} \exp\left(\frac{p_T w_1}{4} \right) \int_{p_T(1+w_1)/4}^{\infty} \exp\left(-\frac{x_3}{2} - \sqrt{4x_3^2 - p_T^2 w_1} \right) \frac{dx_3}{\sqrt{4x_3^2 - p_T^2 w_1}}, \tag{34}$$

$$(1 - k_0) C_i \int_{-\infty}^{t} \int_{-\infty}^{\infty} \int_{-\infty}^{\infty} G_C(\mathbf{p}^{\zeta} | \mathbf{p}_1) dt_1 dx_1 dy_1 = \frac{p_C w_1}{2} \exp\left(\frac{p_C w_1}{4} \right) \int_{p_C(1+w_1)/4}^{\infty} \exp\left(-\frac{x_3}{2} - \sqrt{4x_3^2 - p_C^2 w_1} \right) \frac{dx_3}{\sqrt{4x_3^2 - p_C^2 w_1}}. \tag{35}$$

The final CBIE for the paraboloid of revolution is

$$\begin{aligned} &p_T \exp(p_T) \int_{p_T}^{\infty} \frac{\exp(-x)}{x} dx - \Delta + \frac{d_c K V}{2D_T} - C_i - \frac{Q m_2}{m_1^2 c_p} C_i^2 + 2^n \beta = p_T^2 \exp(p_T) \\ &\times \int_{1}^{\infty} \left(\exp\left(p_T \int_{1}^{w_1} v_2(w_2) dw_2 - \frac{3 p_T w_1}{4} \right) v_2(w_1) \int_{p_T(1+w_1)/4}^{\infty} \exp\left(-\frac{x_3}{2} - \sqrt{4x_3^2 - p_T^2 w_1} \right) \frac{dx_3}{\sqrt{4x_3^2 - p_T^2 w_1}} \right) dw_1, \end{aligned} \tag{36}$$

$$\begin{aligned} C_i = &\frac{C_\infty}{1 - p_C \exp(p_C) \int_{p_C}^{\infty} \frac{\exp(-x)}{x} dx} + \frac{p_C^2 \exp(p_C)}{1 - p_C \exp(p_C) \int_{p_C}^{\infty} \frac{\exp(-x)}{x} dx} \\ &\times \int_{1}^{\infty} \left(\exp\left(p_C \int_{1}^{w_1} v_2(w_2) dw_2 - \frac{3 p_C w_1}{4} \right) v_2(w_1) \int_{p_C(1+w_1)/4}^{\infty} \exp\left(-\frac{x_3}{2} - \sqrt{4x_3^2 - p_C^2 w_1} \right) \frac{dx_3}{\sqrt{4x_3^2 - p_C^2 w_1}} \right) dw_1. \end{aligned} \tag{37}$$

3 | SELECTION OF STABLE GROWTH MODE FOR A DENDRITIC CRYSTAL AND CALCULATION EXAMPLES

A stable growth mode occurs when the selection parameter $\sigma^* = 2d_0 D_T/(\rho^2 V)$ for the three-dimensional crystal growth in temperature and concentration fields reads as [40]

$$\begin{aligned} \sigma^* &= \frac{\sigma_0 \alpha_d^{7/4}}{1 + b\left(\alpha \alpha_d^{-3/4} \right)^{11/14}} \left[\frac{1}{\left(1 + a_1 \sqrt{\alpha_d} p_T \right)^2} - \frac{1}{\left(1 + a_2 \sqrt{\alpha_d} p_T D_T / D_C \right)^2} \frac{2 m_1 C_i (1 - k_0) D_T}{(Q/c_p) D_C} \right], \\ \alpha &= \left(\frac{a d_0 U_\infty}{4\rho V} + \frac{a d_0 U_\infty D_T}{2\rho V D_C} \right) \left(1 - \frac{2 m_1 C_i (1 - k_0) D_T}{D_C Q / c_p} \right), \; a(\mathrm{Re}) = \frac{\exp(-\mathrm{Re}/2)}{E_1(\mathrm{Re}/2)}, \end{aligned} \tag{38}$$

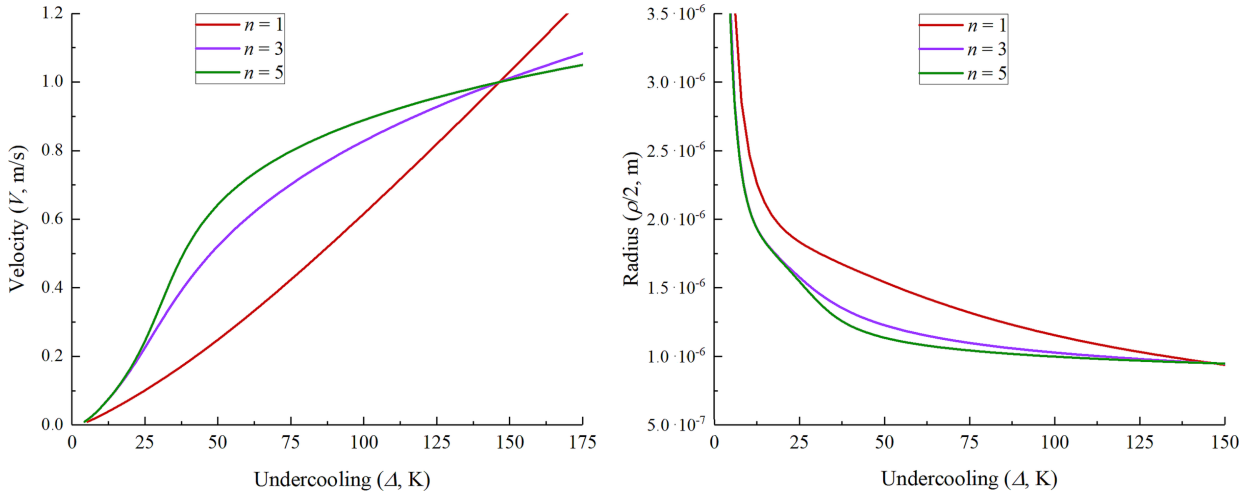

FIGURE 2 Dendrite tip velocity V and radius $\rho/2$ as functions of the melt undercooling Δ for pure $Ni_{99}Zr_1$ alloy without flow ($U_\infty = 0$). The colored lines represent the effect of different powers of the atomic kinetics exponent n. Parameters used in calculation: solidification temperature $T_0' = 1728$ K, hypercooling $Q/c_p = 395$ K, temperature diffusivity $D_T = 1.2 \cdot 10^{-5}$ m^2 s^{-1}, liquidus slope $m_1 = -8.0$ K (at.%)$^{-1}$ and $m_2 = -4.0$ K (at.%)$^{-2}$, diffusion coefficient in liquid $D_C = 2.1 \cdot 10^{-9}$ m^2 s^{-1}, impurity concentration $C_\infty' = 1$ at.%, capillary length $d_c \approx d_0 = 2.02 \cdot 10^{-10}$ m, kinetic coefficient $\beta_k = 0.01$ K (s/m)^n, surface energy anisotropy $\varepsilon_c = 0.017$, selection constant $\sigma_0 = 0.05$. [Colour figure can be viewed at wileyonlinelibrary.com]

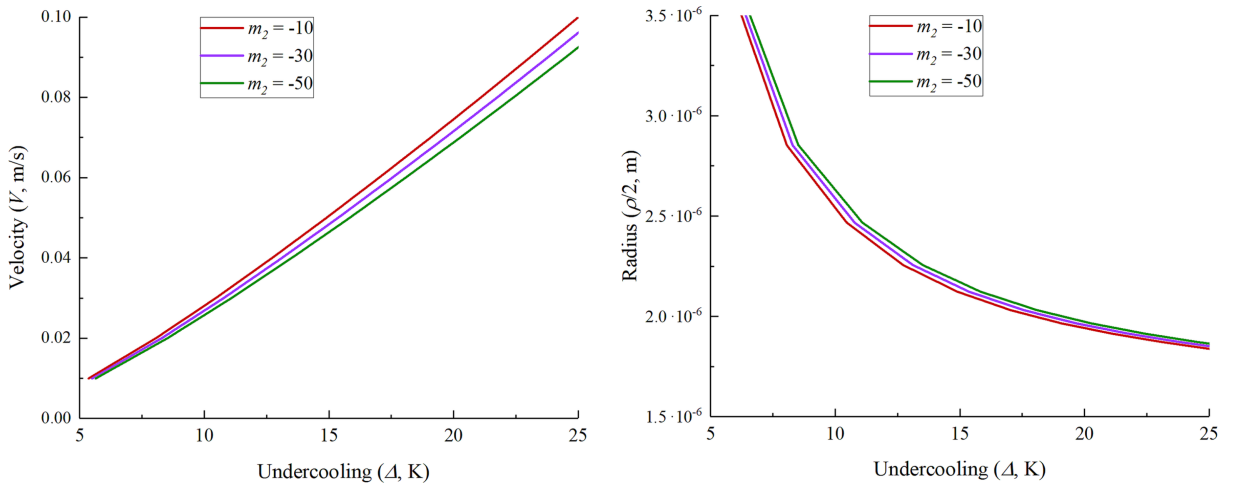

FIGURE 3 Dendrite tip velocity V and radius $\rho/2$ as functions of the melt undercooling Δ for pure $Ni_{99}Zr_1$ alloy without flow ($U_\infty = 0$). The colored lines represent the effect of quadratic liquidus m_2. Physical parameters used for calculations correspond to Figure 3, power of the atomic kinetics exponent $n = 1$ and the coefficient m_2 shown in the figure inserts is measured in K (at.%)$^{-2}$. [Colour figure can be viewed at wileyonlinelibrary.com]

where σ_0 is the selection parameter, b is the second selection constant defining the role of incoming fluid current, $a_1 = (8\sigma_0/7)^{1/2}(3/56)^{3/8}$, $a_2 = \sqrt{2}a_1$, $\alpha_d = 15\varepsilon_c$, and ε_c is the anisotropy of surface energy. Expression (38) defines a sustained growth pattern moving with a constant rate in an undercooled two-component melt in the presence of a fluid current. Generally speaking, the first contribution in square brackets determines the influence of thermal field, the second contribution stems from dissolved impurity, the contribution with constant b characterizes a fluid current, the contributions with the Péclet numbers p_T are responsible for fast solidification scenario. Note that expression (38) is valid for small and intermediate Péclet numbers in local-equilibrium crystallization processes. In the opposite case of fast solidification (great growth rates and Péclet numbers), another selection relation takes place [33, 41].

How the exponent n of attachment kinetics of particles to the phase interface influences the main dependencies $V(\Delta)$ and $\rho(\Delta)/2$ is shown in Figure 2. A change in the degree index n leads to a change in the mechanism of attaching atoms to the crystal. An increase in n leads to an enhancement of the influence of kinetics, which is characteristic of high-rate

solidification at large undercoolings. Our calculations demonstrate that the tip velocity V can vary by up to 50% (red and green lines for $\Delta = 75$ K, left panel). Hence, a great influence of the attachment kinetics of particles on solidification rate takes place. In addition, the tip radius can vary by up to 20% (red and green lines for $\Delta = 50$ K, right panel). How the nonlinear liquidus contribution (proportional to m_2) influences the main dependencies $V(\Delta)$ and $\rho(\Delta)/2$ is shown in Figure 2. As one might think, the growth rate V increases and the tip radius $\rho/2$ decreases when liquid undercooling increases. In addition, V and ρ respectively become smaller and larger when the departure from a linear dependence (coefficient $|m_2|$) of liquidus increases with concentration. Namely, taking the liquid undercooling $\Delta = 25$ K (left panel in Figure 3), we estimate that the tip velocity can vary by up to 10%. Such changes in V and ρ lead to changes in the material microstructure (e.g., the primary interdendritic spacing [42–45]).

In summary, the BIE discussed in this study characterizes a wider class of solidified two-component melts in the presence of a mobile solid-liquid front than earlier derived boundary integral equations. This is due to the fact that the present analysis takes nonlinear form of the phase diagram into account (nonlinear concentration and atomic attachment contributions).

4 | CONCLUSION

In this paper, the boundary integral method for thermo-solutal solidification problem with an arbitrary curvilinear crystallization front is developed with allowance for the nonlinear dependence of the phase transition temperature on solute concentration and the kinetics of atomic attachment at the interface. This equation taking a forced melt flow into account is deduced by means of the Green's function technique previously developed for thermal and concentration moving-boundary problems. The new BIE represents the integro-differential equation for the interface function defining a surface that divides pure solid and liquid materials during crystallization processes. Therefore, the BIE derived describes the evolutionary behavior of growing solid phase patterns (dendrites) in two-component undercooled melts. In addition, our theory describes various shapes met in crystal growth applications as well as the evolution of morphological perturbations that lead to the evolution of secondary crystal branches and complex materials structures [46].

An important research direction related to the development of the BIE theory is the simultaneous consideration of directional interface motion deep into the melt and volumetric crystal growth in front of this boundary. Such an analysis, which takes into account the partial removal of undercooling by crystal growth, should be based on a combination of this theory and the theory of volumetric crystallization [47–55]. Another important area of research is the derivation of BIEs for directional solidification with a mushy region when two moving boundaries exist: “solid phase - mushy region” and “mushy region - liquid phase.” Such a problem should be solved by combining the present approach with a two-phase region theory [56–63].

ACKNOWLEDGEMENTS

The present research work consists of theoretical and computational parts, which were supported by different financial sources. The authors gratefully acknowledge research funding from the Ministry of Science and Higher Education of the Russian Federation (project 075-02-2023-935 for the development of the regional scientific and educational mathematical center “Ural Mathematical Center”) for the theoretical part. LVT thanks the Foundation for the Advancement of Theoretical Physics and Mathematics “BASIS” (project No. 21-1-3-11-1) for the financial support of computational calculations and research studies. Open Access funding enabled and organized by Projekt DEAL.

CONFLICT OF INTEREST STATEMENT

The authors declare no potential conflict of interests.

ORCID

E. A. Titova https://orcid.org/0000-0002-9118-2027
A. A. Ivanov https://orcid.org/0000-0002-2490-160X
L. V. Toropova https://orcid.org/0000-0003-4587-2630

REFERENCES

1. P. Pelcé, *Dynamics of curved fronts*, Academic Press, 1988.
2. W. Kurz and R. Fisher, *Fundamentals of solidification*, Trans. Tech. Publ., 1989.
3. D. V. Alexandrov and A. Y. Zubarev, *Patterns in soft and biological matters*, Phil. Trans. R. Soc. A **378** (2020), 20200002.
4. L. V. Toropova and D. V. Alexandrov, *Dynamical law of the phase interface motion in the presence of crystals nucleation*, Sci. Rep. **12** (2022), no. 1, 10997.
5. D. V. Alexandrov and L. V. Toropova, *The role of incoming flow on crystallization of undercooled liquids with a two-phase layer*, Sci. Rep. **12** (2022), no. 1, 17857.
6. P. K. Galenko, L. V. Toropova, D. V. Alexandrov, G. Phanikumar, H. Assadi, M. Reinartz, P. Paul, Y. Fang, and S. Lippmann, *Anomalous kinetics, patterns formation in recalescence, and final microstructure of rapidly solidified Al-rich Al-Ni alloys*, Acta Mater. **241** (2022), 118384.
7. M. Reinartz, M. Kolbe, M. Herlach, M. Rettenmayr, L. V. Toropova, D. V. Alexandrov, and P. K. Galenko, *Study on anomalous rapid solidification of Al-35 at%Ni in microgravity*, JOM **74** (2022), no. 6, 2420–2427.
8. D. V. Alexandrov and A. Y. Zubarev, *Transport phenomena in complex systems (part 2)*, Phil. Trans. R. Soc. A **380** (2022), 20210366.
9. E. V. Makoveeva, D. V. Alexandrov, and A. A. Ivanov, *On the theory of unsteady-state operation of bulk continuous crystallization*, Crystals **12** (2022), 1634.
10. W. W. Mullins and R. F. Sekerka, *Stability of a planar interface during solidification of a dilute binary alloy*, J. Appl. Phys. **35** (1964), 444–451.
11. P. Bouissou and P. Pelcé, *Effect of a forced flow on dendritic growth*, Phys. Rev. A **40** (1989), 6637–6680.
12. D. V. Alexandrov, *Self-similar solidification: morphological stability of the regime*, Int. J. Heat Mass Trans. **47** (2004), 1383–1389.
13. D. V. Alexandrov and A. P. Malygin, *Convective instability of directional crystallization in a forced flow: The role of brine channels in a mushy layer on nonlinear dynamics of binary systems*, Int. J. Heat Mass Trans. **54** (2011), 1144–1149.
14. D. V. Alexandrov and A. P. Malygin, *Flow-induced morphological instability and solidification with the slurry and mushy layers in the presence of convection*, Int. J. Heat Mass Trans. **55** (2012), 3196–3204.
15. R. N. Hills, D. E. Loper, and P. H. Roberts, *A thermodynamically consistent model of a mushy zone*, Q. J. Appl. Math. **36** (1983), 505–539.
16. M. G. Worster, *Solidification of an alloy from a cooled boundary*, J. Fluid Mech. **167** (1986), 481–501.
17. I. V. Alexandrova, D. V. Alexandrov, D. L. Aseev, and S. V. Bulitcheva, *Mushy layer formation during solidification of binary alloys from a cooled wall: the role of boundary conditions*, Acta Physica Polonica A **115** (2009), 791–794.
18. I. G. Nizovtseva and D. V. Alexandrov, *The effect of density changes on crystallization with a mushy layer*, Phil. Trans. R. Soc. A **378** (2020), 20190248.
19. L. V. Toropova, A. A. Ivanov, S. I. Osipov, Y. Yang, E. V. Makoveeva, and D. V. Alexandrov, *Solidification of ternary melts with a two-phase layer*, J. Phys.: Condens. Matter **34** (2022), 383002.
20. D. Herlach, P. Galenko, and D. Holland-Moritz, *Metastable solids from undercooled melts*, Elsevier, 2007.
21. P. K. Galenko and D. V. Alexandrov, *From atomistic interfaces to dendritic patterns*, Phil. Trans. R. Soc. A **376** (2018), 20170210.
22. D. V. Alexandrov and A. Y. Zubarev, *Heterogeneous materials: metastable and non-ergodic internal structures*, Phil. Trans. R. Soc. A **377** (2019), 20180353.
23. D. V. Alexandrov and P. K. Galenko, *Dendritic growth with the six-fold symmetry: theoretical predictions and experimental verification*, J. Phys. Chem. Solids **108** (2017), 98–103.
24. G. E. Nash, *Capillary-limited, steady state dendritic growth: I. Theoretical development*, 1974. NRL Report 7679.
25. G. E. Nash and M. E. Glicksman, *Capillary-limited steady-state dendritic growth: I. Theoretical development*, Acta Metall. **22** (1974), 1283–1290.
26. J. S. Langer and L. A. Turski, *Studies in the theory of interfacial stability: I. Stationary symmetric model*, Acta Metall. **25** (1977), 1113–1119.
27. J. S. Langer, *Studies in the theory of interfacial stability: II. Moving symmetric model*, Acta Metall. **25** (1977), 1121–1137.
28. D. V. Alexandrov and P. K. Galenko, *Boundary integral approach for propagating interfaces in a binary non-isothermal mixture*, Physica A **469** (2017), 420–428.
29. P. K. Galenko, D. V. Alexandrov, and E. A. Titova, *The boundary integral theory for slow and rapid curved solid/liquid interfaces propagating into binary systems*, Phil. Trans. R. Soc. A **376** (2018), 20170218.
30. D. A. Saville and P. J. Beaghton, *Growth of needle-shaped crystals in the presence of convection*, Phys. Rev. A **37** (1988), 3423–3430.
31. E. A. Titova and D. V. Alexandrov, *The boundary integral equation for curved solid/liquid interfaces propagating into a binary liquid with convection*, J. Phys. A: Math. Theor. **55** (2022), 055701.
32. E. A. Titova and D. V. Alexandrov, *Analysis of the boundary integral equation for the growth of a parabolic/paraboloidal dendrite with convection*, J. Phys.: Condens. Matter **34** (2022), 244002.
33. D. V. Alexandrov and P. K. Galenko, *Selected mode for rapidly growing needle-like dendrite controlled by heat and mass transport*, Acta Mater. **137** (2017), 64–70.
34. M. N. Barber, A. Barbieri, and J. S. Langer, *Dynamics of dendritic sidebranching in the two-dimensional symmetric model of solidification*, Phys. Rev. A **36** (1987), 3340–3349.
35. E. A. Brener and V. I. Mel'nikov, *Pattern selection in two-dimensional dendritic growth*, Adv. Phys. **40** (1991), 53–97.
36. D. V. Alexandrov, I. V. Rakhmatullina, and A. P. Malygin, *On the theory of solidification with a two-phase concentration supercooling zone*, Russian Metallurgy (Metally) **2010** (2010), no. 8, 745–750.
37. P. M. Morse and H. Feshbach, *Methods of theoretical physics*, McGraw-Hill, 1953.
38. I. S. Gradshteyn and I. M. Ryzhik, *Tables of integrals, series, and products*, Academic, 2007.

39. S. K. Dash and W. N. Gill, *Foced convection heat and momentum transfer to dendritic structures (parabolic cylinders and paraboloids of revolution)*, Int. J. Heat Mass Trans. **27** (1984), 1345–1356.
40. D. V. Alexandrov and P. K. Galenko, *A review on the theory of stable dendritic growth*, Phil. Trans. R. Soc. A **379** (2021), 20200325.
41. D. V. Alexandrov and P. K. Galenko, *Selection criterion of stable mode of dendritic growth with n-fold symmetry at arbitrary Péclet numbers with a forced convection*, Iutam bookseries, Vol. **34**, 2019, pp. 203–215.
42. R. Deguen, T. Alboussière, and D. Brito, *On the existence and structure of a mush at the inner core boundary of the earth*, Phys. Earth Planet. Int. **164** (2007), 36–49.
43. D. V. Alexandrov and A. V. Britousova, *Interdendritic spacing in growth processes with a mushy layer*, AIP Confer. Proc. **1648** (2014), 850101.
44. L. V. Toropova, D. V. Alexandrov, M. Rettenmayr, and D. Liu, *Microstructure and morphology of Si crystals grown in pure Si and Al-Si melts*, J. Phys. Condens. Matter **34** (2022), no. 8, 094002.
45. L. V. Toropova, *Shape functions for dendrite tips of SCN and Si*, Eur. Phys. J. Special Topics **231** (2022), no. 6, 1129–1133.
46. D. V. Alexandrov and P. K. Galenko, *The shape of dendritic tips*, Phil. Trans. R. Soc. A **378** (2020), 20190243.
47. Y. A. Buyevich and V. V. Mansurov, *Kinetics of the intermediate stage of phase transition in batch crystallization*, J. Cryst. Growth **104** (1990), 861–867.
48. Y. A. Buyevich, Y. M. Goldobin, and G. P. Yasnikov, *Evolution of a particulate system governed by exchange with its environment*, Int. J. Heat Mass Trans. **37** (1994), 3003–3014.
49. E. V. Makoveeva and D. V. Alexandrov, *On the theory of phase transformation process in a binary supercooled melt*, Eur. Phys. J. Spec. Top. **229** (2020), 375–382.
50. E. V. Makoveeva and D. V. Alexandrov, *Mathematical simulation of the crystal nucleation and growth at the intermediate stage of a phase transition*, Russian Metallurgy (Metally) **2018** (2018), no. 8, 707–715.
51. D. A. Barlow, *Theory of the intermediate stage of crystal growth with applications to protein crystallization*, J. Cryst. Growth **311** (2009), 2480–2483.
52. D. A. Barlow, *Theory of the intermediate stage of crystal growth with applications to insulin crystallization*, J. Cryst. Growth **470** (2017), 8–14.
53. D. V. Alexandrov, *Nonlinear dynamics of polydisperse assemblages of particles evolving in metastable media*, Eur. Phys. J. Spec. Top. **229** (2020), 383–404.
54. E. V. Makoveeva and D. V. Alexandrov, *The bulk crystal growth in binary supercooled melts with allowance for heat removal*, Eur. Phys. J. Spec. Top. **231** (2022), 1101–1106.
55. E. V. Makoveeva, D. V. Alexandrov, and S. P. Fedotov, *Analysis of smoluchowski's coagulation equation with injection*, Crystals **12** (2022), 1159.
56. A. C. Fowler, *The formation of freckles in binary alloys*, IMA J. Appl. Math. **35** (1985), 159–174.
57. R. C. Kerr, A. W. Woods, M. G. Worster, and H. E. Huppert, *Solidification of an alloy cooled from above. Part 1. Equilibrium growth*, J. Fluid Mech. **216** (1990), 323–342.
58. D. V. Alexandrov, *Solidification with a quasiequilibrium mushy region: exact analytical solution of nonlinear model*, J. Cryst. Growth **222** (2001), 816–821.
59. D. V. Alexandrov, D. L. Aseev, I. G. Nizovtseva, H.-N. Huang, and D. Lee, *Nonlinear dynamics of directional solidification with a mushy layer. analytic solutions of the problem*, Int. J. Heat Mass Trans. **50** (2007), 3616–3623.
60. D. V. Alexandrov, I. G. Nizovtseva, A. P. Malygin, H.-N. Huang, and D. Lee, *Unidirectional solidification of binary melts from a cooled boundary: analytical solutions of a nonlinear diffusion-limited problem*, J. Phys.: Condens. Matter **20** (2008), 114105.
61. L. V. Toropova, D. L. Aseev, S. I. Osipov, and A. A. Ivanov, *Mathematical modeling of bulk and directional crystallization with the moving phase transition layer*, Math. Methods Appl. Sci. **45** (2022), no. 13, 8011–8021.
62. D. V. Alexandrov, I. A. Bashkirtseva, and L. B. Ryashko, *Nonlinear dynamics of mushy layers induced by external stochastic fluctuations*, Phil. Trans. R. Soc. A **376** (2018), 20170216.
63. L. V. Toropova, E. V. Makoveeva, S. I. Osipov, A. P. Malygin, Y. Yang, and D. V. Alexandrov, *Nucleation and growth of an ensemble of crystals during the intermediate stage of a phase transition in metastable liquids*, Crystals **12** (2022), 895.

How to cite this article: E. A. Titova, A. A. Ivanov, and L. V. Toropova, *The boundary integral equation describing a curvilinear solid/liquid interface with nonlinear phase transition temperature*, Math. Meth. Appl. Sci. (2023), 1–11, DOI 10.1002/mma.9520.